Received: 24 July

Analyzing population dynamics of Indian Ocean albacore (*Thunnus alalunga*) using Bayesian state-space production model

Bai Li[1,2], Jie Cao[1,2], Jiangfeng Zhu[1]

[1]National Engineering Research Center for Oceanic Fisheries, Shanghai Ocean Univeristy, 999 Hucheng Huan Road, Shanghai 201306, China
[2]School of Marine Sciences, University of Maine, Orono, ME, 04469, U.S.

Abstract
A Bayesian state-space production model was developed to assess the stock status of Indian Ocean albacore (*Thunnus alalunga*) using fishery data from 1950 to 2014. The first scenario (S1) used total catch and two standardized CPUE from the Southwest region 3 (1979-2014) and the Southeast region 4 (1979-2005). The second scenario (S2) used total catch and one CPUE from the Southwest region 3 to model the population dynamics of Indian Ocean albacore. The results from the S1 showed that the mean of Maximum Sustainable Yield (MSY; 1000 t), B_{2014}/B_{MSY}, and F_{2014}/F_{MSY} were 48.41, 1.49, and 0.51. The results from the S2 indicated that the mean of MSY (1000 t), B_{2014}/B_{MSY}, and F_{2014}/F_{MSY} were 48.66, 1.47, and 0.50. The estimated parameters from S1 and S2 showed well convergence. A continued exploration of sensitivity analyses, risk assessment, and retrospective analyses may improve the uncertainty of current models

1. Introduction
The stock population dynamics of Indian Ocean albacore (*Thunnus alalunga*) has previously been assessed using ASPIC (Matsumoto et al., 2014) and Bayesian biomass dynamics model (Guan et al., 2014). The Bayesian approach is able to model uncertainty about key population parameters. However, this approach does not account for the randomness in the dynamics of the population. To improve the assessment by modeling the randomness in both the dynamics of the population (e.g. process error) and in the observations made on the population (e.g. observation error), a state-space paradigm was applied to a Bayesian production model (Millar and Meyer, 2000). In this study, a Bayesian state-space formulation of the Schaefer surplus production model was used to analyze population dynamics of Indian Ocean albacore. The Bayesian state-space production model (BSP) was built from the winBUGS and R platforms to compare results with other stock assessment models.

2. Data
Four areas with independent catch and standardized CPUE time series were available for the assessment of Albacore (e.g. area 1-Northwest, area 2-Northeast, area 3-Southwest, and area 4-Southeast) from the WPTmT06. The catch data were obtained from IOTC-2016-WPTmT-DATA-SA.xlsx (available at http://www.iotc.org/meetings/6th-working-party-temperate-tunas-wptmt06). The corresponding standardized CPUE, which were developed by considering vessel ID factor from 1979 to 2014, were also obtained through the website of the WPTmT06.

Figure 1. Historical catch (t) from four areas used by BSP model.

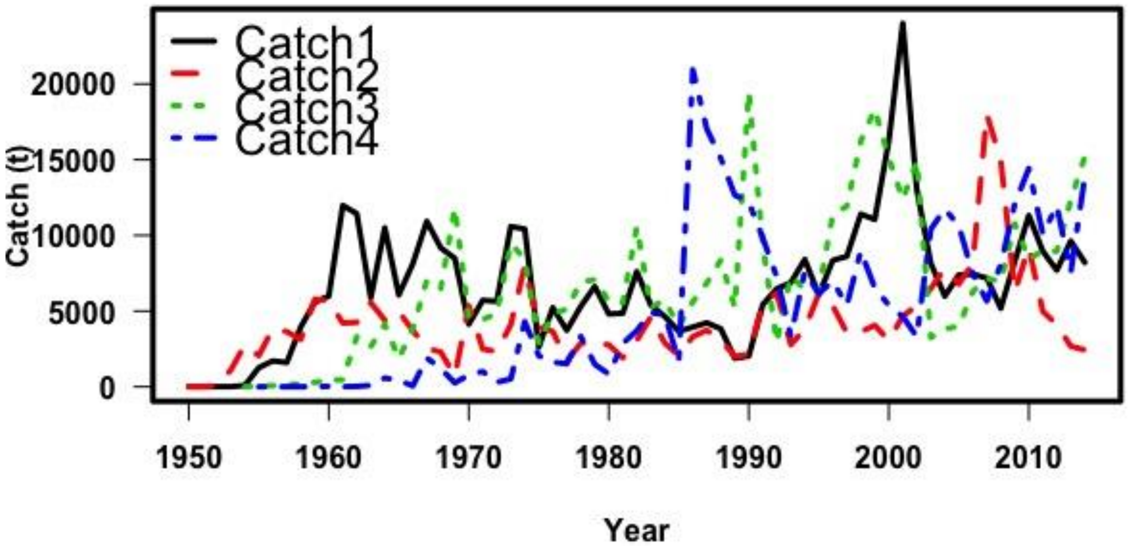

Figure 2. Standardized CPUE from four areas used by BSP model.

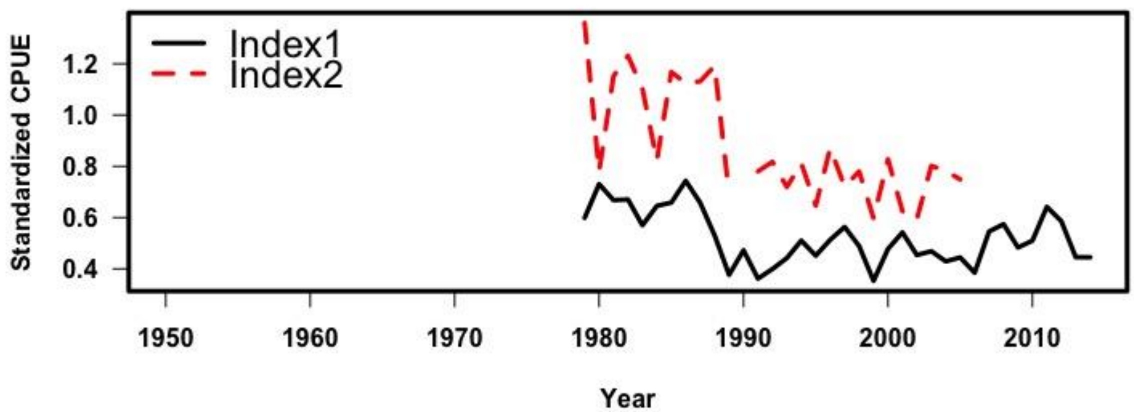

3. Bayesian state-space production model

The Bayesian state-space production model was formulated by considering both observation and process errors. The observation error likelihood function measures the discrepancy between observed and predicted CPUE (Millar and Meyer, 2000). The process error accounts for the fluctuations in exploitable albacore biomass due to density-dependent processes and fishery harvests (WCPFC, 2014). The biomass in year t (B_t) depends on the previous biomass (B_{t-1}), catch (C_{t-1}), intrinsic growth rate (r), carrying capacity (K), and a production shape parameter (s):

$$B_t = B_{t-1} + r \times B_{t-1}\left(1 - \left(\frac{B_{t-1}}{K}\right)^s\right) - C_{t-1}$$
(1)

In order to improve the efficiency of estimating parameters, the equation (1) was re-parameterized using the proportion of carrying capacity (P=B/K). The process error terms were assumed to be independent and log-normally distributed random variable $exp(\mu_1)$ with mean 0 and variance σ^2:

$$P_1 = exp(\mu_1) \quad (2)$$

$$P_t = (P_{t-1} + r \times P_{t-1}(1 - P_{t-1}^s) - \frac{C_{t-1}}{K})exp(u_t) \quad \text{for } t > 1 \quad (3)$$

The observation error terms assumed that each CPUE index (I) was proportional to biomass with catchability coefficient q. The observation error was independent and log-normally distributed variable exp(v_t) with mean 0 and variance τ^2:

$$I_t = q_I B_t = q_I K P_t v_t \quad (4)$$

The BMSY, FMSY, and MSY were estimated by using the following equations (WCPFC, 2014):

$$B_{MSY} = K \times (s+1)^{-\frac{1}{s}} \quad (5)$$

$$F_{MSY} = -log(1 - r \times (1 - \frac{1}{s+1})) \quad (6)$$

$$MSY = r \times (1 - \frac{1}{s+1}) \times K \times (s+1)^{-\frac{1}{s}} \quad (7)$$

The prior distributions of each parameter were given in Table 1. Most of the prior distribution was set with a uniform distribution. The model was run with two scenarios that are denoted as S1 and S2 in Table 1.

Table 1. Prior distribution of parameters used in Bayesian state-space production model.

Scenario	CPUE Series	r	K	P1	1/q	σ	τ	s
S1	R3, R4	U[0.01, 1.5]	U[2, 32]	U[1, 10]	U[1,1000]	Gamma(4, 0.01)	Gamma(2, 0.01)	U[0.01, 2]
S2	R3	U[0.01, 1.5]	U[2, 32]	U[1, 10]	U[1,1000]	Gamma(4, 0.01)	Gamma(2, 0.01)	U[0.01, 2]

Notes: S1 and S2 represented different combinations of CPUE series. R3 and R4 represented CPUE from southwest and southeast regions. U and Gamma represented uniform and gamma distribution respectively. K was scaled by the maximum annual catch.

4. Results

The mean and standard deviation of the posterior distributions were summarized in the Table 2. The Brooks-Gelman-Rubin statistic was used to diagnose the convergence. The model was converged if the convergence index is close to 1 and less than 1.1. The convergence values indicated that all parameters beside K from the S1 have well convergence with the rhat less than 1.1. The K is marginal converged with a value of 1.14. Posterior density distributions of model parameters for each scenario were given from Figure 3 and 10. The scatter plot of r, K, q for different scenarios indicated strong correlation between K and q (Figure 4 and 11). The process error was low and fluctuated around 0 (Figure 5 and 12). The modeled indices showed a similar pattern with process error from the start year of the index (Figure 7 and 12). The Bratio (B/B_{MSY}) for all scenarios showed a similar trend (Figure 8 and 13). The value of Bratio decreased dramatically from the first year to the second year, and stayed stable for later years. The Fratio (F/F_{MSY}) was low for the entire time series with a relatively high upper boundary of 95% CI (Figure 8 and 13). The Kobe plots showed that the stock was not overfished and overfishing was not occurring for both scenarios (Figure 9 and 14).

Table 2. Estimated mean, standard deviation (sd), 95% CI, median, and convergence of parameters.

	Scenarios	**Mean**	**sd**	**2.50%**	**50%**	**97.50%**	**Convergence**
r	**S1**	0.7091	0.3838	0.13	0.6532	1.448	1.00
	S2	0.7395	0.3779	0.1584	0.6919	1.452	1.00
K (1000 t)	**S1**	550.7	165.7	296.9	536.9	1020	1.14
	S2	501.2	143.9	244.6	497.9	826.3	1.00
P1	**S1**	2.765	1.214	1.082	2.581	5.387	1.00
	S2	2.734	1.226	1.073	2.526	5.435	1.00
q	**S1_q1**	0.001364	3.70E-04	0.001008	0.001242	0.002362	1.00
	S1_q2	0.002251	6.19E-04	0.001616	0.002054	0.00393	1.00
	S2	0.001514	5.42E-04	0.001012	0.001348	0.003077	1.04
σ	**S1**	0.02208	0.01037	0.007881	0.02014	0.04747	1.00
	S2	0.02637	0.01156	0.009534	0.02449	0.05448	1.00
τ	**S1_ τ1**	0.0128	0.006724	0.002946	0.01174	0.02902	1.00
	S1_ τ2	0.03497	0.01448	0.01518	0.03224	0.07127	1.00
	S2	0.01064	0.006783	0.001639	0.009244	0.02722	1.00
s	**S1**	0.6376	0.4261	0.1248	0.5093	1.764	1.00
	S2	0.6548	0.4153	0.1404	0.5341	1.745	1.00
MSY (1000 t)	**S1**	48.41	16.49	20.36	46.3	85.98	1.01
	S2	48.66	16.43	21.6	46.61	86.34	1.00

Figure 3. Posterior distribution of parameters for S1.

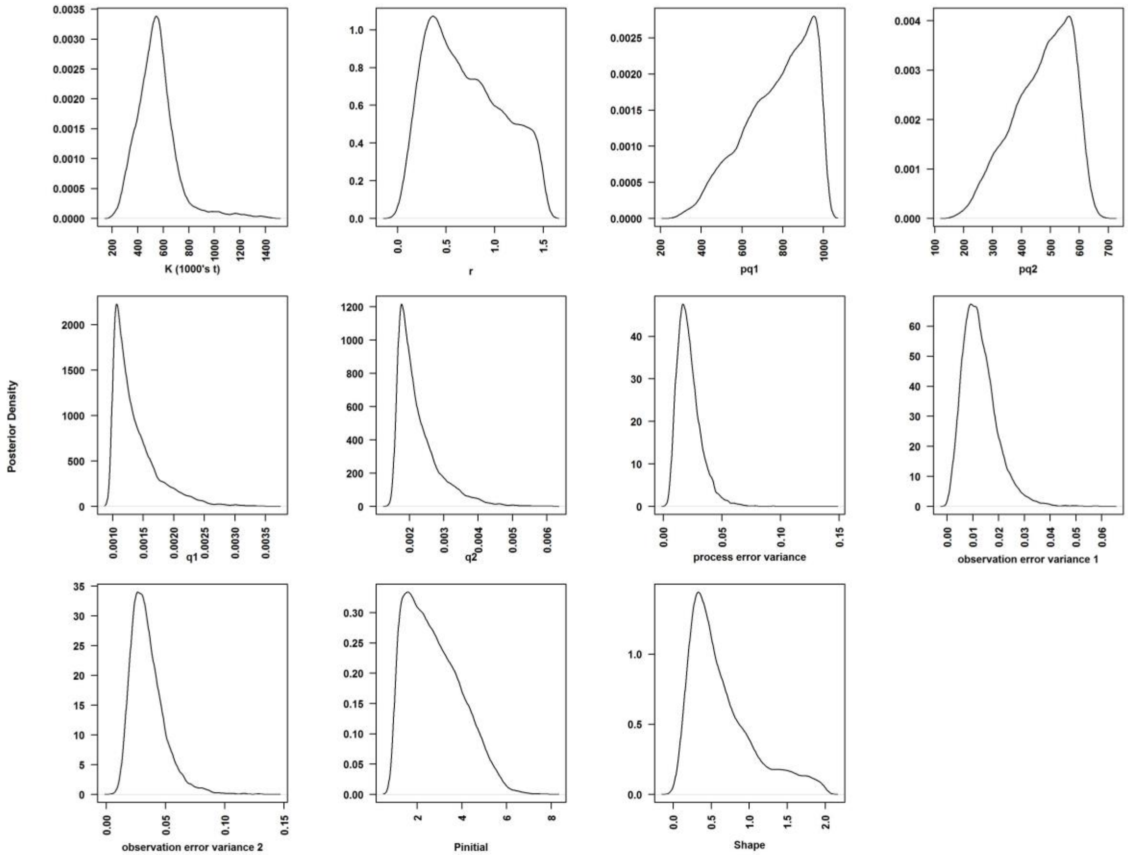

Figure 4. Relationships between r, K, q from S1.

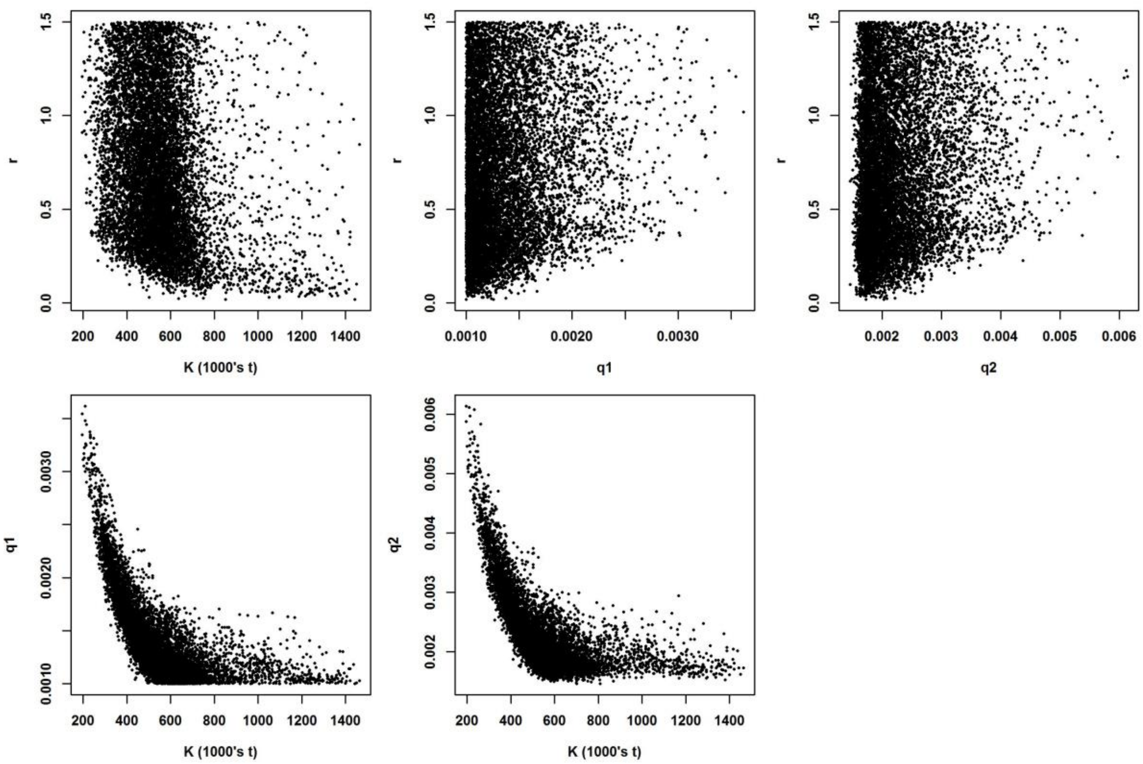

Figure 5. Process errors from S1 change as function of years. The solid black line represents mean, and the dash lines are 95% CI.

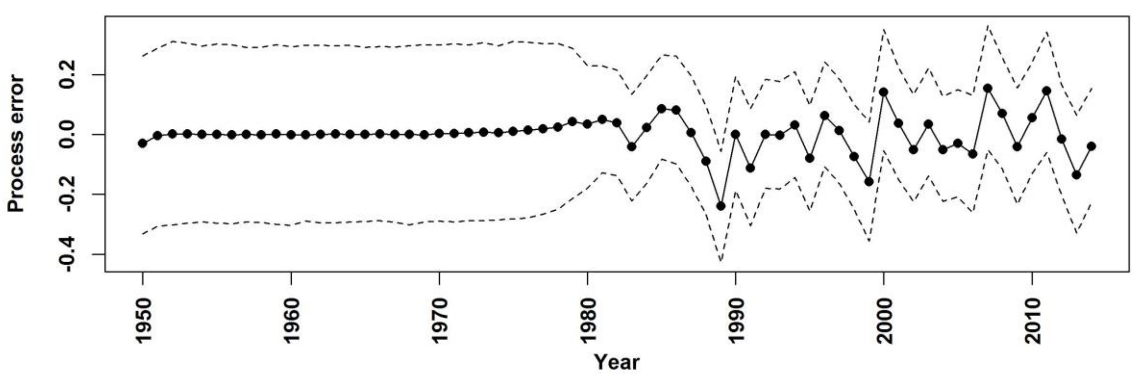

Figure 6. Modeled indices from S1 change as function of years. The solid black line represents mean, and the dash lines are 95% CI.

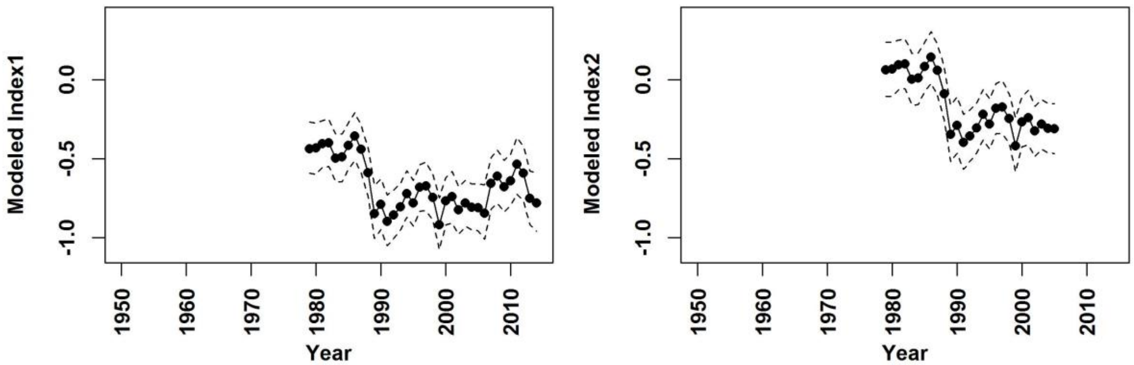

Figure 7. Modeled indices residuals from S1 change as function of years. The solid black line represents mean, and the dash lines are 95% CI.

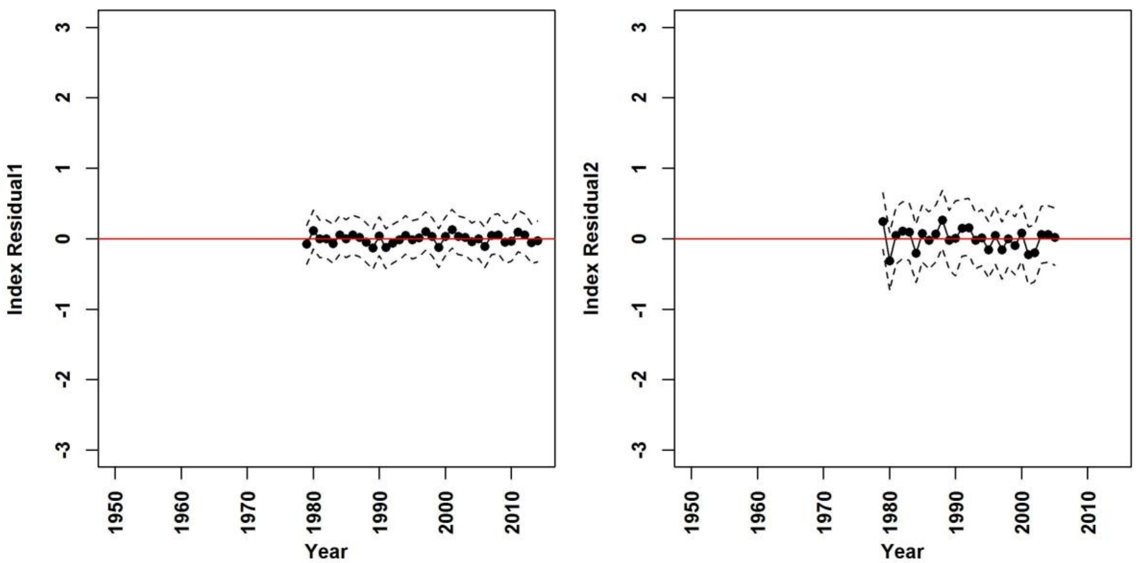

Figure 8. Changes over time in Bratio and Fratio from S1. The solid black line represents mean, and the dash lines are 95% CI.

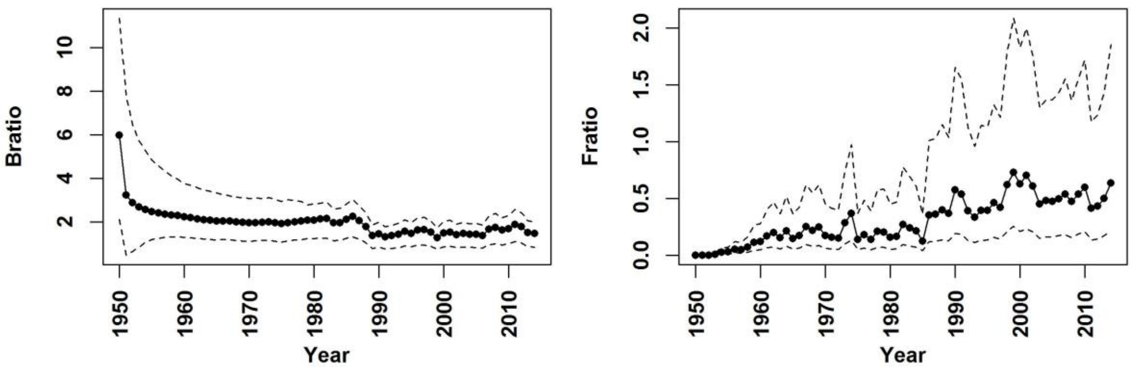

Figure 9. The Kobe plot for S1. The red point represents the fishery status in 2014.

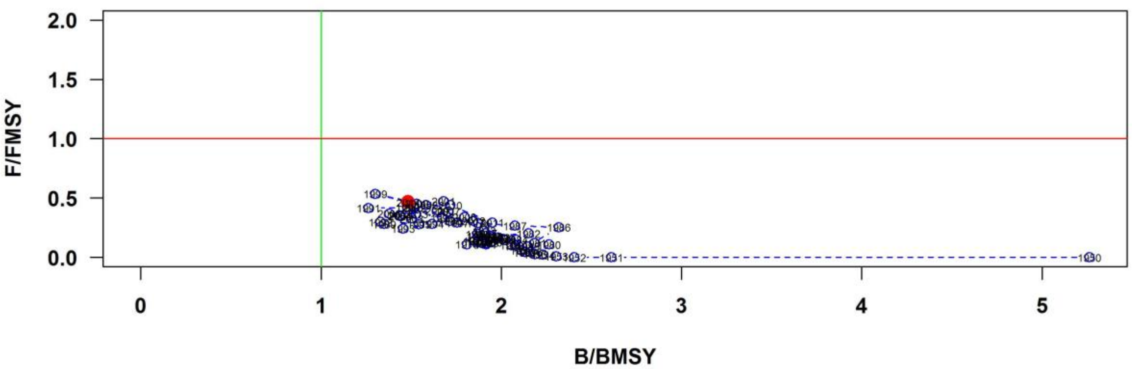

Figure 10. Posterior distribution of parameters for S2.

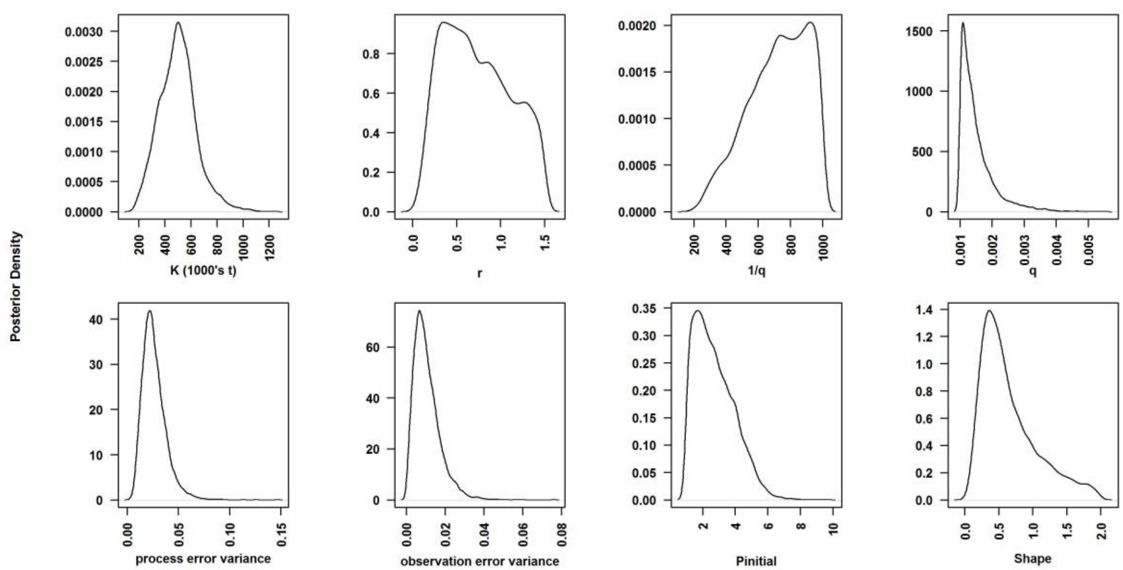

Figure 11. Relationships between r, K, q from S2.

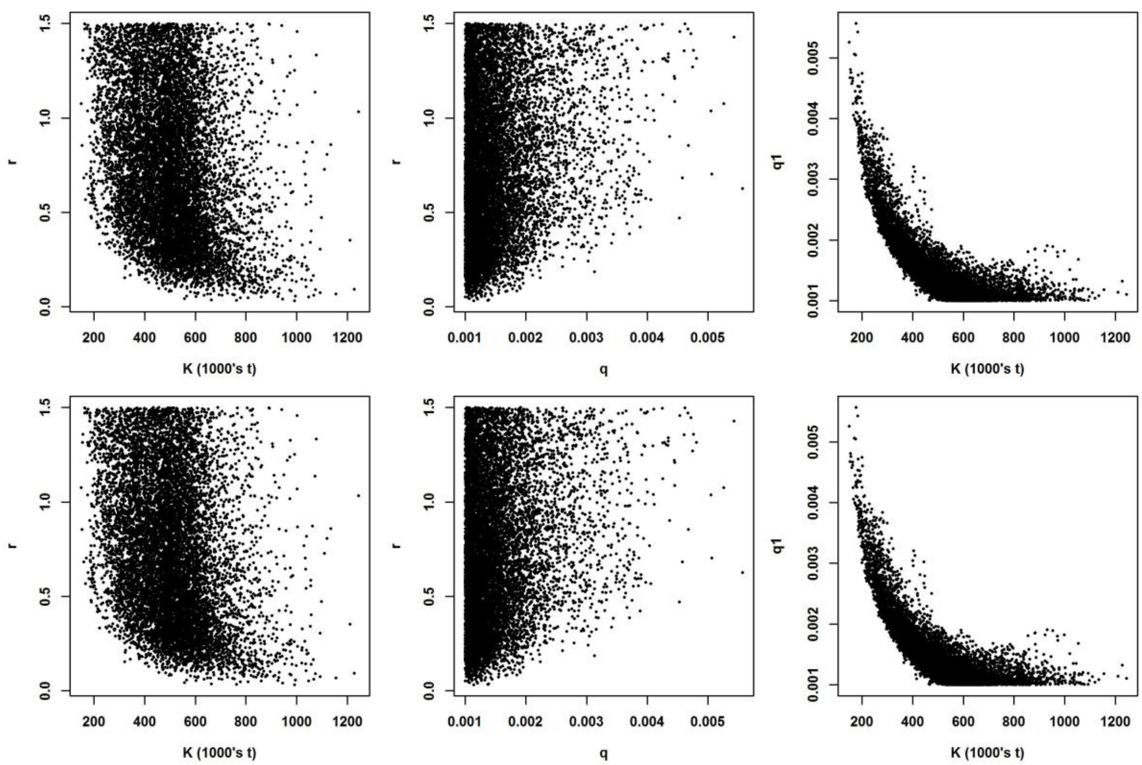

Figure 12. Process error, modeled index, and index residuals from S2 change as function of year. The solid black line represents mean, and the dash lines are 95% CI.

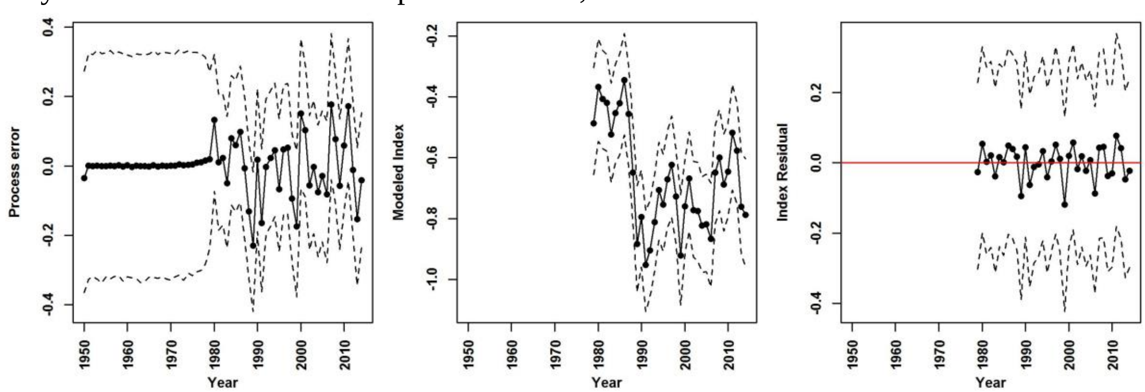

Figure 13. Changes over time in Bratio and Fratio from S2. The solid black line represents mean, and the dash lines are 95% CI.

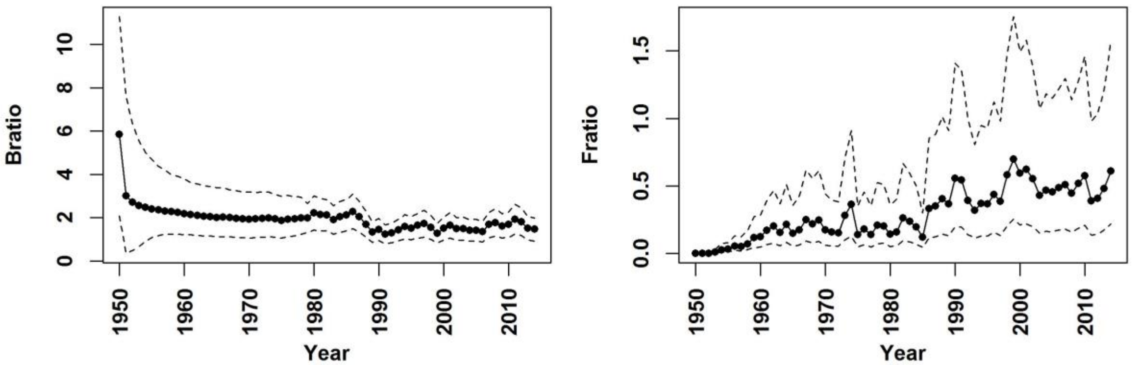

Figure 14. The Kobe plot for S2. The red point represents the fishery status in 2014.

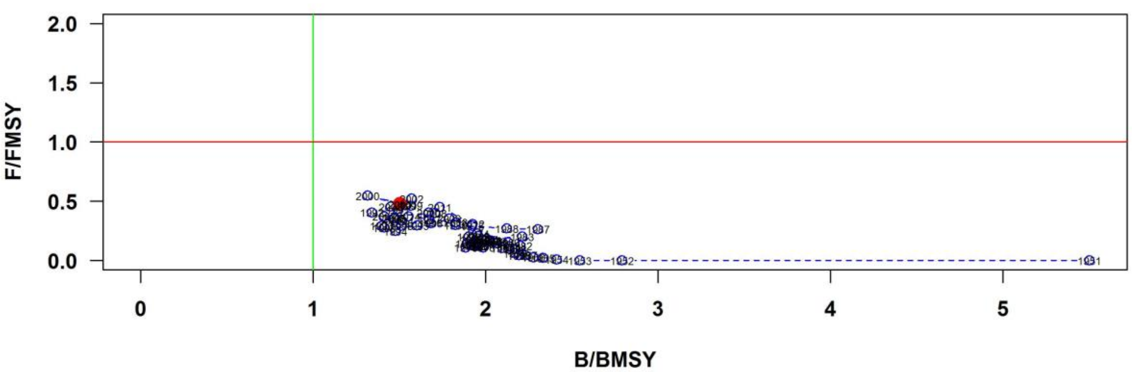

Acknowledgement

The work was supported by the Project of GaoFeng Discipline of Fishery Science and International Center for Marine Studies at Shanghai Ocean University.

References

Guan, W., Tang, L., Zhu, J., Tian, S., and Xu, L. 2016. Application of a Bayesian method to data-poor stock assessment by using Indian Ocean albacore (*Thunnus alalunga*) stock assessment as an example. Acta Oceanologica Sinica, 35(2): 117-125. doi: 10.1007/s13131-016-0814-0.

Matsumoto, T., Nishida, T., and Kitakado, T. 2014. Stock and risk assessments of albacore in the Indian Ocean based on ASPIC. IOTC-2014-WPTmT05-22.

Millar, R.B., and Meyer, R. 2000. Non-linear state space modelling of fisheries biomass dynamics by using Metropolis-Hastings within-Gibbs sampling. Journal of the Royal Statistical Society. 49(3): 327-342.

WCPFC. 2014. North Pacific swordfish (*Xiphiaus gladius*) stock assessment in 2014: Annex 9.